Consistent hybrid LES-FDF formulation for the simulation of turbulent combustion

By V. Raman, H. Pitsch AND R. O. Fox †

1. Motivation and objectives

The numerical simulation of turbulent reactive flows is a complex and challenging problem with widespread practical use. Recent breakthroughs in algorithmic techniques and the drastic increase in computing power have provided us with the tools to understand the complex interaction between turbulence and chemical reactions. In the past decade, the use of the large-eddy simulation (LES) technique has made it possible to make accurate predictions of turbulent flows even for complex configurations. On the other hand, the treatment of combustion is mainly through models similar to that used in the Reynolds-Averaged NS methods (RANS) like flamelet models or conditional moment closure type approximations. Although these models work well for systems that exhibit little or no extinction, a higher-dimensional multi-scalar model is required to describe slow and extinction chemistry. The transported-filtered density function (FDF) (Colucci *et al.* 1998) method provides a natural starting point for such detailed description. The FDF technique has the key advantage that the reaction source term of the scalars appears closed and requires no modeling.

Though a joint velocity-composition FDF transport equation can be formulated, numerical implementations of this high-dimensional system pose stability and feasibility issues. To overcome this problem, a hybrid approach is used where the velocity and turbulence fields are solved using an Eulerian scheme (like RANS or LES), while the scalar transport is handled using the FDF approach. Although the FDF technique has been widely used in the RANS context, almost all the applications involve steady-state flows. Since LES is inherently transient, the coupled LES-FDF method needs to maintain temporal accuracy. Due to the statistical nature of the FDF scheme, such a coupled scheme poses numerical accuracy issues.

Hence, in order to establish the accuracy of a LES-FDF implementation, a robust consistency criterion is formulated. Based on redundant density fields carried by the Eulerian as well as the Lagrangian part of the solver, it is required that the evolution of all such density fields should be equivalent. The theoretical development guarantees such an equivalence. The current implementation of the LES-FDF scheme is then used to verify this equivalence in the context of a numerical simulation of a variable density complex flow problem.

2. Hybrid LES-FDF scheme

In the hybrid scheme implemented here, the LES technique is based on a low-Mach number approximation-based finite-volume scheme. Further details of the LES implementation can be found elsewhere (Pierce 2001; Pierce & Moin 2004). The Lagrangian method uses stochastic particles to evolve the FDF.

† Iowa State University

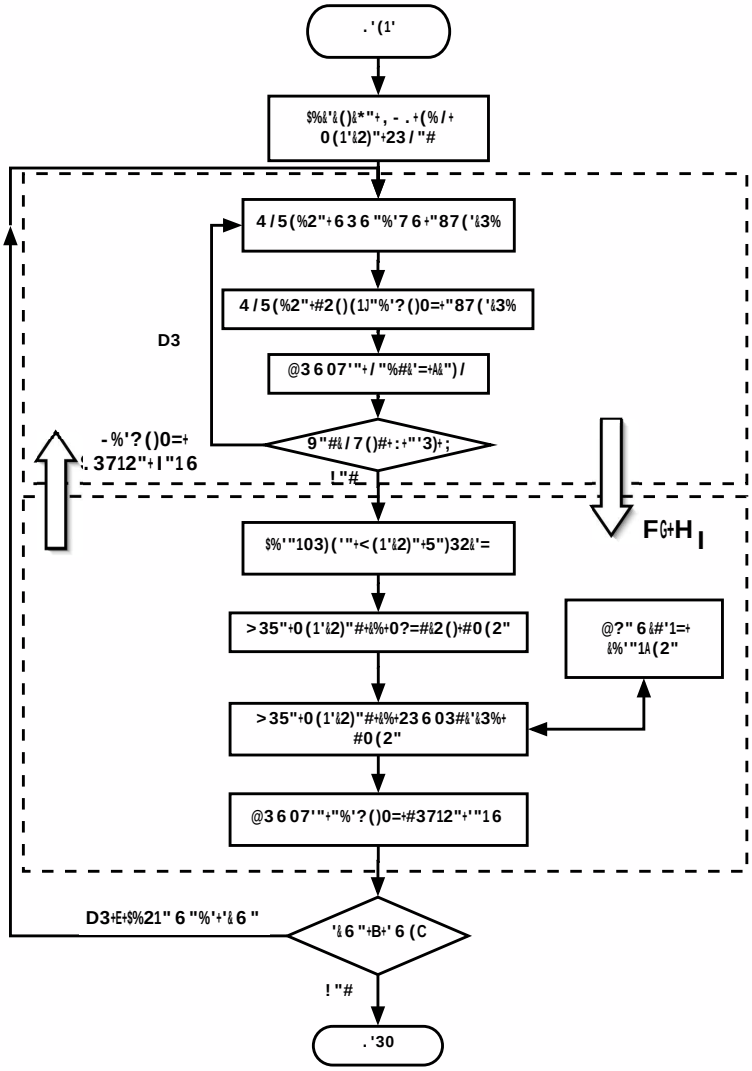

FIGURE 1. Flowchart showing the coupled LES-FDF simulation with feedback.

The particle method is obtained from the fundamental FDF transport equation. The FDF in a variable density flow can be defined as:

$$F_L(\boldsymbol{\psi};\mathbf{x},t) = \int_{-\infty}^{+\infty} \rho(\mathbf{y},t)\,\xi[\boldsymbol{\psi},\boldsymbol{\phi}(\mathbf{y},t)]\,G(\mathbf{y}-\mathbf{x})\,d\mathbf{y}, \tag{2.1}$$

$$\xi[\boldsymbol{\psi},\boldsymbol{\phi}(\mathbf{y},t)] = \delta[\boldsymbol{\psi}-\boldsymbol{\phi}(\mathbf{y},t)], \tag{2.2}$$

where δ is an N-dimensional delta function for an N-species system and $\boldsymbol{\psi}$ is the sample space variable in the composition domain. The FDF definition yields the following property:

$$\int_{-\infty}^{+\infty} F_L\,d\boldsymbol{\psi} = \int_{-\infty}^{+\infty} \rho(\mathbf{y},t)\,G(\mathbf{y}-\mathbf{x})\,d\mathbf{y} = \overline{\rho}. \tag{2.3}$$

Similarly, the filtered mean of any scalar Q_ϕ can be defined as:

$$\widetilde{Q_\phi} = \int_{-\infty}^{+\infty} Q_\phi(\boldsymbol{\psi}, \mathbf{y}, t) F_L d\boldsymbol{\psi} = \frac{1}{\overline{\rho}} \int_{-\infty}^{+\infty} \rho(\mathbf{y}, t)\, Q_\phi(\mathbf{y}, t)\, G(\mathbf{y} - \mathbf{x})\, d\mathbf{y}. \tag{2.4}$$

Using these definitions, the transport equation for the joint composition FDF can be written as (Colucci *et al.* 1998; Jaberi *et al.* 1999)

$$\frac{\partial F_L}{\partial t} + \frac{\partial}{\partial \mathbf{x}}(\widetilde{\mathbf{u}} F_L) + \frac{\partial}{\partial \mathbf{x}}\left(\widetilde{\mathbf{u}'|\boldsymbol{\psi}} F_L\right) = -\frac{\partial}{\partial \boldsymbol{\psi}}\left[\left(\frac{1}{\overline{\rho}}\overline{\nabla \cdot \rho D \nabla \boldsymbol{\phi}|\boldsymbol{\psi}} + \mathbf{S}(\boldsymbol{\psi})\right) F_L\right], \tag{2.5}$$

where $\widetilde{\mathbf{u}}$ is the filtered velocity field, $\widetilde{\mathbf{u}'|\boldsymbol{\psi}}$ is the sub-filter velocity fluctuation conditioned on the scalar, $\overline{\nabla \cdot \rho D \nabla \boldsymbol{\phi}|\boldsymbol{\psi}}$ is the conditional micromixing term, and $\mathbf{S}$ is the reaction source term. The conditional velocity term is modeled using the gradient-diffusion hypothesis to give

$$\widetilde{u_i'|\boldsymbol{\psi}} F_L = -\overline{\rho} D_T \frac{\partial F_L/\rho}{\partial x_i}. \tag{2.6}$$

The conditional mixing term is closed using the Interaction-by-Exchange-with-the-Mean (IEM) model (Villermaux 1986).

$$\overline{\nabla \cdot \rho D \nabla \boldsymbol{\phi}|\boldsymbol{\psi}} = \nabla \cdot \overline{\rho} D \nabla \widetilde{\boldsymbol{\phi}} - \frac{\overline{\rho} C_\phi}{\tau}\left(\boldsymbol{\psi} - \widetilde{\boldsymbol{\phi}}\right), \tag{2.7}$$

where C_ϕ is scalar-to-mechanical time-scale ratio and τ is a turbulence time scale. In the present study we set $C_\phi = 2$ (Peters 2000) and use a turbulent-diffusivity-based time scale (Colucci *et al.* 1998).

The high dimensionality of the FDF equation makes finite-differencing-based solution techniques infeasible. A stochastic approach (Pope 2000) is used where the filtered momentum equations are solved using conventional grid-based techniques (like LES) while the FDF equation is solved using a particle-based Monte-Carlo approach. The Lagrangian approach uses a large ensemble of notional particles to represent the fluid. These particles evolve using a set of stochastic differential equations obtained from the above FDF transport equation. The stochastic differential equations are functions of the filtered LES flow fields. Hence, the Lagrangian system uses the filtered fields from the LES solver to advance the notional particles. Using the particle properties, mean fields are constructed that are fed back to the LES solver. The LES solver then advances the flow using these mean fields. Figure 1 shows the flowchart of the hybrid algorithm.

Typically, the Lagrangian system provides the filtered density field that is then used by the LES solver. However, the stochastic nature of the FDF scheme leads to large statistical fluctuations in the filtered density field. Direct feedback of this noisy field usually leads to numerical instabilities. Here, to increase the robustness of the feedback algorithm, an additional enthalpy equation is used. Following (Muradoglu *et al.* 1999), we define the equivalent enthalpy, h as

$$h(\boldsymbol{\psi}) = \frac{\gamma}{\gamma - 1}\frac{P_0}{\rho(\boldsymbol{\psi})}, \tag{2.8}$$

where γ is the ratio of the specific heats, P_0 is the operating pressure. Since the equivalent enthalpy is only a function of the local thermochemical composition, the transport equation for h can be derived from the FDF transport equation.

$$\frac{\partial \overline{\rho}\widetilde{h}}{\partial t} + \frac{\partial}{\partial \mathbf{x}}\left(\overline{\rho}\widetilde{\mathbf{u}}\widetilde{h}\right) = \frac{\partial}{\partial \mathbf{x}}\left(\overline{\rho}(D + D_T)\frac{\partial \widetilde{h}}{\partial \mathbf{x}}\right) + \overline{\rho}\left(\widetilde{h_\alpha S_\alpha} - \frac{1}{2\tau} C_\phi \overline{\rho} \widetilde{h_\alpha \phi''_\alpha}\right), \tag{2.9}$$

$$h_\alpha = \frac{\partial h}{\partial \phi_\alpha}, \tag{2.10}$$

where α represents the components of the N-dimensional composition array. It is evident that the physical transport terms in this equation can be treated in the same way as a conserved scalar equation. The source terms, however, are not known and need to be provided by the FDF solver. In terms of the particle properties, the source term is the change of enthalpy of the particles due to reaction and mixing (Muradoglu *et al.* 1999):

$$\widetilde{S_h} = \overline{\rho}\left(\widetilde{h_\alpha S_\alpha} - \frac{1}{2\tau} C_\phi \overline{\rho} h_\alpha \widetilde{\phi''}_\alpha\right). \tag{2.11}$$

Once the equivalent enthalpy is known, the density field is found using the relation obtained by filtering Eq. 2.8:

$$\overline{\rho} = \frac{\gamma}{\gamma - 1}\frac{P_0}{\widetilde{h}}, \tag{2.12}$$

where the low-Mach number assumption has been used to remove the pressure fluctuations. This density field is then used to advance the LES flow solver. It is found that this feedback mechanism is numerically stable and does not lead to large spikes in the $d\overline{\rho}/dt$ term that appears in the continuity equation.

To increase statistical accuracy, large particle numbers are needed making such methods computationally expensive. Numerical implementation of the LES-FDF scheme is an algorithmic challenge and novel techniques are used to reduce the computational expense of these schemes (Raman *et al.* 2004). A major issue in such implementations is to consistently couple a stochastic FDF scheme and a deterministic Eulerian scheme. Though steady-state-based flow solvers have been successfully used (Muradoglu *et al.* 1999), a consistent algorithm for a temporally variant system (like the LES-based approach) has not been studied in detail so far. Here we propose a criterion for a consistent implementation and test it with a challenging reacting flow problem.

3. Consistency requirements

In the Lagrangian particle-based system, the computational domain is decomposed into a large number of notional particles that represent the fluid. The particles are initially distributed uniformly and evolve in space and time using stochastic differential equations (Pope 2000). Each particle carries information about its location, a composition vector and a representative weight. In order to pass information from and to the LES solver, particle mean fields are obtained by a weighted summation process involving particle properties in a given computational cell. The particle weight is initially assigned to be a fraction of the local fluid mass such that the sum of the particle weights in a computational cell equals the cell fluid mass.

$$w_k = \frac{V_i \overline{\rho}_i}{N_p}, \tag{3.1}$$

where w_k is the particle weight, V_i is the cell volume, $\overline{\rho}_i$ is the fluid density in cell i, and N_p is the number of particles in the cell. As the particles evolve with time, the sum of the weights of the particles in a given cell is dependent on the enforcement of the continuity equation. The particle weight has no direct evolution equation and will follow the particle trajectory. At any time step, the particle-weights based density can be obtained by using the sum of particle weights in a given cell.

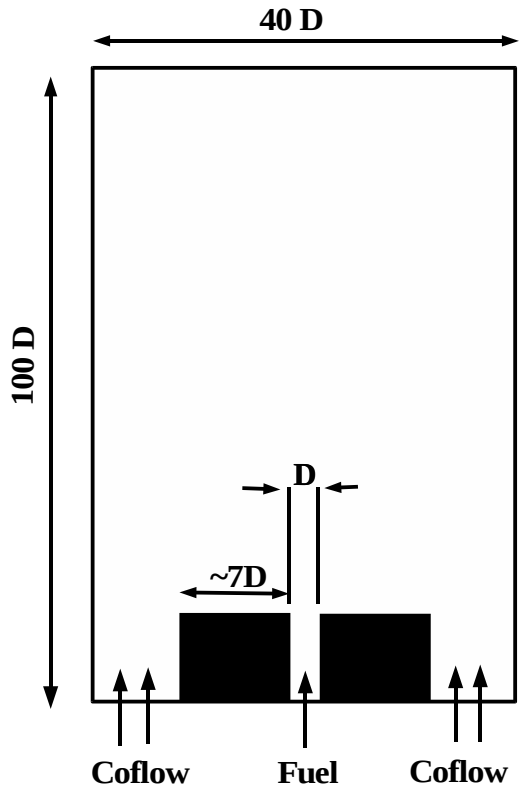

FIGURE 2. Schematic of the bluff-body flame configuration. The jet diameter D is 3.6 mm.

$$\overline{\rho}_w = \frac{1}{V_i} \sum_{i=1}^{N_p} w_k. \tag{3.2}$$

In addition to the particle weight, a mean density can also be obtained from the particle composition vector based on thermochemical properties.

$$\overline{\rho}_p^{-1} = \frac{\sum_{k=1}^{N_p} w_k / \rho\left(\phi_k\right)}{\sum_{k=1}^{N_p} w_k}, \tag{3.3}$$

where $\rho(\phi)$ is the thermochemical density computed using the particle composition. The initial conditions are chosen such that $\overline{\rho} = \overline{\rho}_p$ at $t = 0$. As the particles evolve in space and time, the density fields evolve through different equations, though indirectly, they should all satisfy the continuity equation. By construction (Raman *et al.* 2004), the thermochemical density ($\overline{\rho}_p$) and the LES density ($\overline{\rho}$) evolve closely. This is ensured by solving an ancillary enthalpy transport equation using Eulerian schemes. The source term

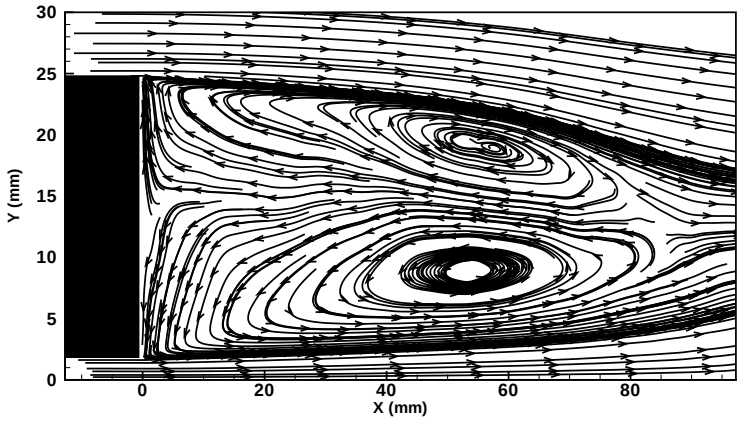

FIGURE 3. Streamtraces of the time-averaged velocity vector showing the counter-rotating vortices.

for the enthalpy equation is provided using the particle properties. The Eulerian density is obtained directly using this enthalpy field (Muradoglu *et al.* 1999).

On the other hand, the particle weights-based density ($\overline{\rho}_w$) evolves with the particle motion. Based on the continuity equation, it can be shown (Pope 2000) that for the particles to be uniformly distributed, the particle-weights-based density should be equivalent to the Eulerian density field. However, the stochastic evolution scheme will make the particle-based mean fields noisy. Hence a strict equality can be obtained only by time-averaging a statistically stationary field. Finite particle number density can also introduce a bias in the mean fields. This will lead to a progressive divergence of the particle-weights-based density field from the Eulerian field. Such a bias will be readily observed through particle agglomeration in certain sections of the grid and depletion of particles in other regions. The sampling error induced by such low particle number density will further increase the error in mean-field estimation.

A consistent algorithm should hence maintain the equivalence of the three density fields described above. It is noted that this amounts to a consistent evolution of the zeroth moment of the FDF-transport equation. The accuracy of the scheme can be tested using higher-order moments of the same equation. For the single-scalar flamelet model used here, the first moment of the scalar can be evolved simultaneously by both the particle and Eulerian systems. Such a moments-based validation procedure ensures a robust yet simple way of demonstrating the accuracy of the numerical implementation. We will illustrate the validation criteria using an experimental flame next.

4. Numerical test

A bluff-body stabilized experimental flame is simulated using the LES-FDF scheme. The methane/hydrogen fuel jet is separated from the coflow of air by a solid body (Fig. 2). The presence of this bluff-body induces strong recirculation zones that stabilize the flame. In fact, time-averaged streamtraces (Fig. 3) show the presence of two counter-rotating vortices that help mix the coflow with the fuel. The interaction of the high-velocity jets with the slow recirculating fluid creates high shear rates where the reaction is controlled predominantly by mixing. This complex unsteady reacting flow makes an ideal candidate

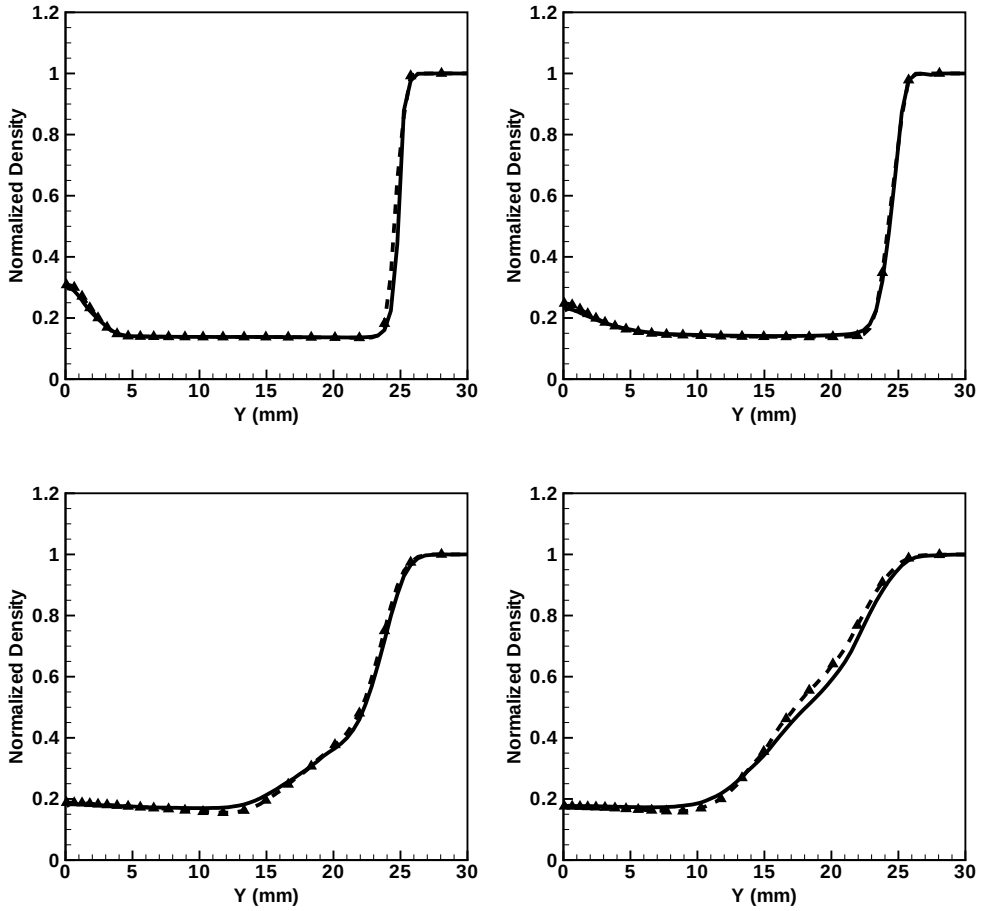

FIGURE 4. Comparison of density obtained from particle weights (dashed line), particle composition (solid line) and LES flow solver (symbols). The four plots are at downstream locations of (top) 13, 30, (bottom) 65, and 90 mm, respectively. The density values have been normalized by the density of the coflow.

for testing the LES-FDF scheme. A computational domain of $256 \times 128 \times 32$ is used along with a nominal particle number density of 15 per cell. Combustion is described using a laminar flamelet chemistry.

The FDF solver was initialized with 15 particles per cell. During the course of the simulation, the total number of particles in the domain was in the range of 10.5–21 million. The simulations were started from cold-flow-converged results, after which the mixture was ignited using the flamelet solution. All simulations were continued for 7 flow-through times, where each flow through time is defined by the time it takes for a particle to travel along the centerline from the inflow to the exit of the domain. The simulation is time-averaged for 1.5 flow-through times starting at two different time-steps separated by 1 flow-through time. The two time-averaged profiles differed by less than 2 % for the mixture-fraction radial profiles ensuring that statistical stationarity has been reached.

The LES-FDF simulation took roughly 200 hours on an 8-processor 600 MHz computer to reach statistical stationarity.

Figure 4 shows time-averaged radial profiles of the three density fields. The density profiles show very good agreement indicating that the FDF implementation is accurate. It was further confirmed that the time-averaged particle number density was constant indicating that there was no long term accumulation of statistical errors. This trend continues at further downstream positions as well.

Figures 5 and 6 show the time-averaged mixture-fraction and RMS mixture-fraction radial profiles at different axial locations. To aid in the comparison, the Eulerian mixture-fraction and RMS mixture-fraction fields obtained from the finite-volume solution of the scalar transport equation are also included. It is observed that the mean mixture-fraction profiles obtained from the FDF solver and the Eulerian solver show excellent agreement with one another and the experimental data as well. The near-bluff-body profile shows a flat profile in the recirculation zone, further affirming the large-scale mixing in this region. The sharp decay of the mixture fraction near the edge of the bluff body is a region of large temperature changes, and consequently large density gradients. At $X = 30\,\mathrm{mm}$, the recirculation region is slightly overpredicted, indicated by the large mixture-fraction values as compared to experiments as well as a sharper decay at the outer vortex signifying a thin reaction zone. Further downstream, the profiles are in much better agreement with the experimental data. At $X = 90\,\mathrm{mm}$, the profiles indicate a tendency of the flame to be narrower than the experimental observation. This is a direct consequence of the grid coarsening to limit the number of computational cells, and leads to the faster decay of the axial velocity.

The RMS profiles show good agreement with experimental data, although certain discrepancies are noticed near the centerline. In general, it is observed that the results agree well with the Eulerian computation as well. At the first axial position considered, the FDF as well as Eulerian calculation show the right RMS profile indicating that the large-scale recirculation has been captured accurately. It is noted that the sub-filter or the unresolved variance in this zone is very small since the large-scale mixing renders the fluid homogeneous. Similar trends are observed at $X = 30$, and $45\,\mathrm{mm}$, but the extent of the recirculation zone in the radial direction decreases as implied by the streamtrace profile (Fig 3). At $X = 65\,\mathrm{mm}$, the secondary peak in the mixture-fraction RMS corresponding to the end of the recirculation zone is captured very accurately. Further downstream, the peak in the RMS profile is shifted towards the centerline which is consistent with the mixture-fraction profiles that indicate a narrower jet spreading than the experimental observation.

It is observed that the RMS profile from the FDF calculation at $X = 30\,\mathrm{mm}$ and $X = 45$ mm show a peak near the centerline that is much larger than the experimental data. One explanation for this behavior is the reduction of accuracy of the particle tracking near the centerline. The LES solver uses a semi-implicit form, where the radial and azimuthal directions are treated implicitly, and are hence independent of the CFL criteria accounting for the radial and azimuthal components. However, the particle method is fully explicit implying that in regions where the CFL criteria computed based on the radial or azimuthal velocity is not satisfied, the errors could be significant. It was found from an analysis of the turbulent-diffusivity profile that such an event is more likely to occur in the region where the central fuel jet breaks down. For this flow, this region varied from $X = 25\,\mathrm{mm}$ to $X = 60\,\mathrm{mm}$. It is noted that the CFL criterion is not violated at each time step, but the additive errors due to frequent violation of this condition led to a spurious

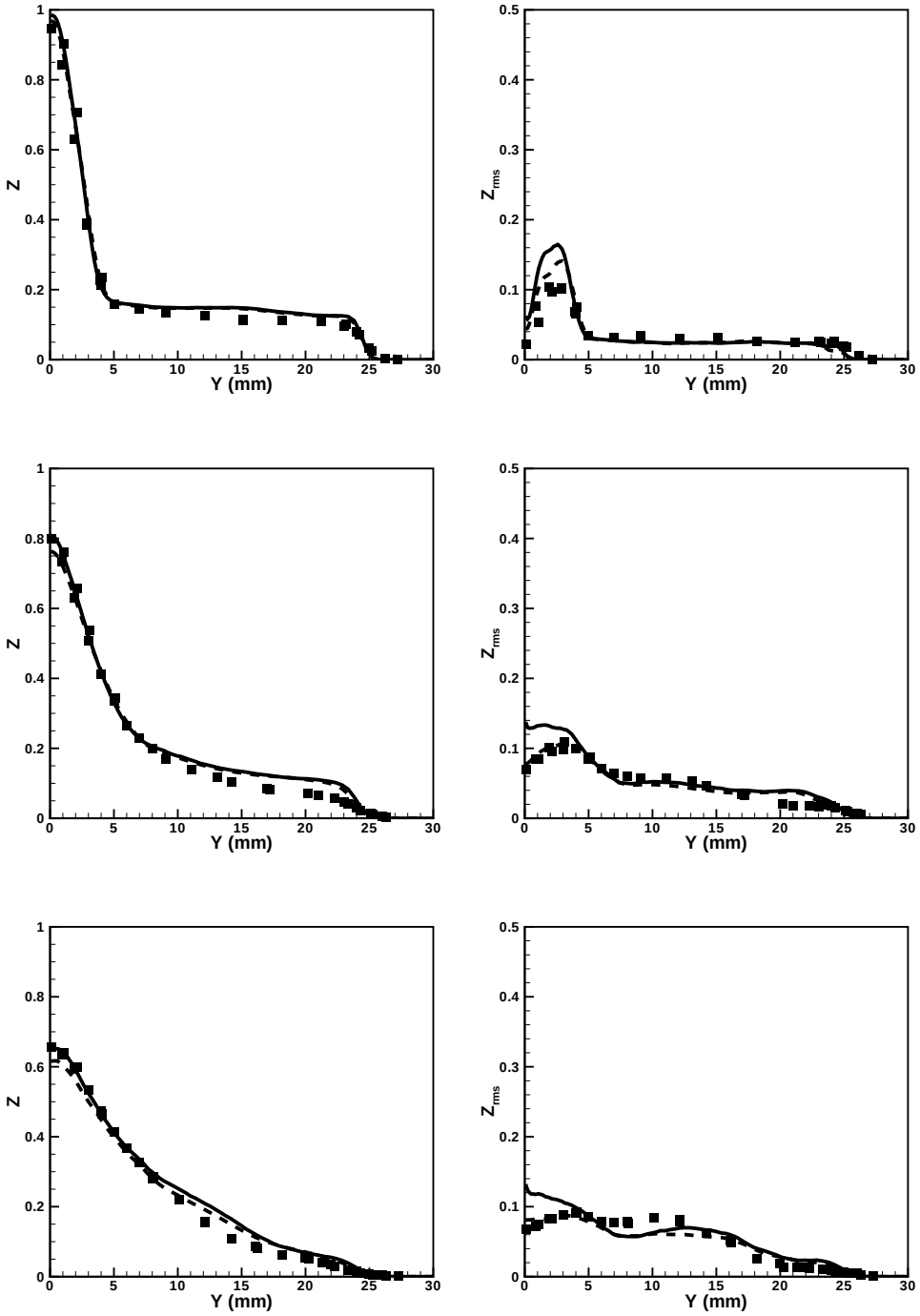

FIGURE 5. Comparison of mean mixture fraction and RMS mixture fraction profiles with experimental data at different axial locations. From top to bottom, $X = 13$, 30, and 45 mm. Symbols are experimental data, solid lines show FDF-based results and dashed lines show beta-function-based Eulerian calculation.

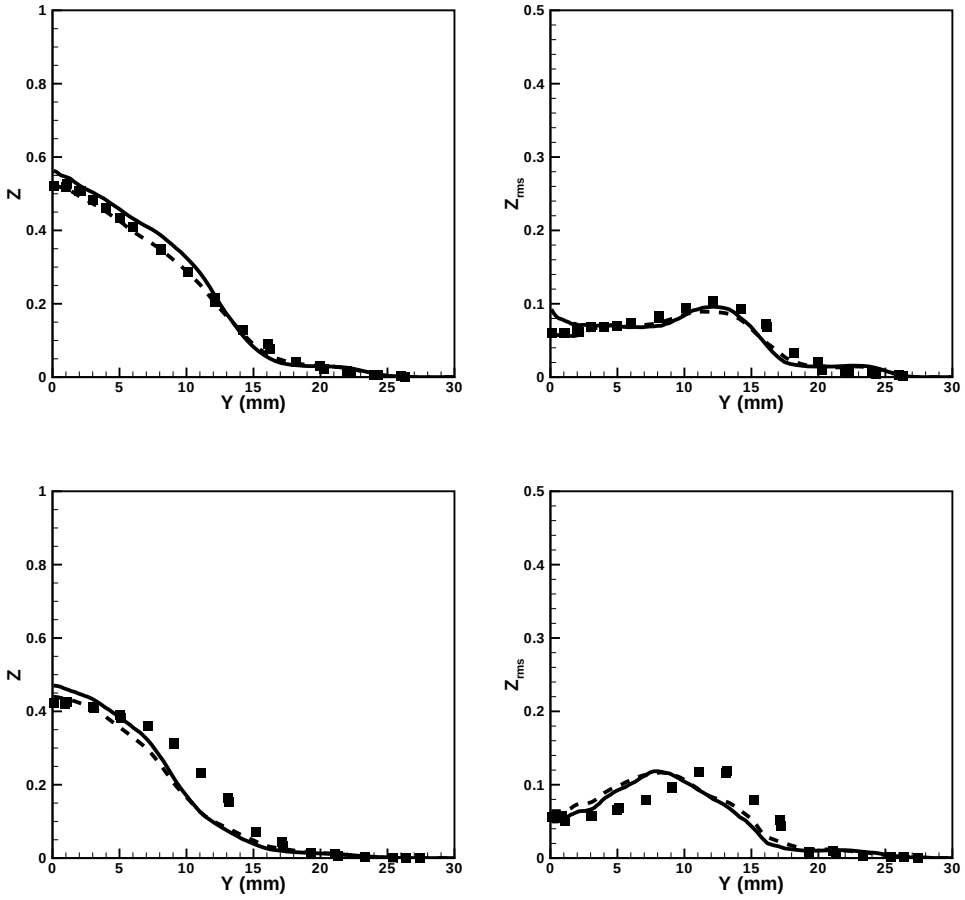

FIGURE 6. Comparison of mean mixture fraction and RMS mixture fraction profiles with experimental data at different axial locations. From top to bottom, $X = 65$ and 90 mm. Symbols are experimental data, solid lines show FDF-based results and dashed lines show beta-function-based Eulerian calculation.

increase in the RMS fluctuation. Since the purpose of this study is to establish the hybrid technique as a viable tool for practical flows, no further evaluations are reported on this observation. Although not reported here, increase in the nominal particle number density decreased this error. Currently, a multi-step fractional-stepping algorithm is being tested to overcome this problem.

5. Conclusion

A consistent hybrid LES-FDF scheme has been developed and implemented for variable density flows. The LES-FDF scheme has been validated by using a density-based consistency condition. An experimental flame configuration was used to test the validation scheme. Currently, direct integration of the chemical source term is being used with a detailed chemical mechanism to fully exploit the advantages of the LES-FDF technique.

REFERENCES

COLUCCI, P. J., JABERI, F. A. & GIVI, P. 1998 Filtered density function for large eddy simulation of turbulent reacting flows. *Physics of Fluids* **10** (2), 499–515.

JABERI, F. A., COLUCCI, P. J., JAMES, S., GIVI, P. & POPE, S. B. 1999 Filtered mass density function for large-eddy simulation of turbulent reacting flows. *Journal of Fluid Mechanics* **401**, 85–121.

MURADOGLU, M., JENNY, P., POPE, S. B. & CAUGHEY, D. A. 1999 A consistent hybrid finite-volume/particle method for the PDF equations of turbulent reactive flows. *Journal of Computational Physics* **154**, 342–371.

PETERS, N. 2000 *Turbulent Combustion*. Cambridge University Press.

PIERCE, C. D. 2001 Progress-variable approach for large-eddy simulation of turbulence combustion. PhD thesis, Stanford University.

PIERCE, C. D. & MOIN, P. 2004 Progress-variable approach for large-eddy simulation of non-premixed turbulent combustion. *Journal of Fluid Mechanics* **504**, 73–97.

POPE, S. B. 2000 *Turbulent Flows*. Cambridge University Press.

RAMAN, V., PITSCH, H. & FOX, R. O. 2004 A consistent hybrid les-fdf scheme for the simulation of turbulent reactive flows. *Submitted to Comb. and Flame*

VILLERMAUX, J. 1986 Micromixing phenomena in stirred reactors. In *Encyclopedia of Fluid Mechanics*, chap. 27. Gulf, Houston, TX.